Measurement of Coolant in a Flat Heat Pipe Using Neutron Radiography

Mizuta, Kei; Saito, Yasushi; Goshima, Takashi; Tsutsui, Toshio

ELSEVIER
CrossMark
Available online at www.sciencedirect.com
ScienceDirect
Physics Procedia 69 (2015) 556 – 563
Physics Procedia

10 World Conference on Neutron Radiography 5-10 October 2014

Measurement of coolant in a flat heat pipe using neutron radiography

Kei Mizuta[a,*], Yasushi Saito[b], Takashi Goshima[a], Toshio Tsutsui[a]

[a] *Department of Chemical Engineering, Kagoshima University, 1-21-40 Korimoto, Kagoshima, Japan*
[b] *Research Reactor Institute, Kyoto University, 2, Asashiro-Nishi, Kumatori-cho, Sennan-gun, Osaka 590-0494 JAPAN*

Abstract

A newly developed flat heat pipe FGHP^{TM} (Morex Kiire Co.) was experimentally investigated by using neutron radiography. The test sample of the FGHP heat spreader was $65 \times 65 \times 2$ mm^3 composed of several etched copper plates and pure water was used as the coolant. Neutron radiography was performed at the E-2 port of the Kyoto University Research Reactor (KUR). The coolant distributions in the wick area of the FGHP and its heat transfer characteristics were measured at heating conditions. Experimental results show that the coolant distributions depend slightly on its installation posture and that the liquid thickness in the wick region remains constant with increasing heat input to the FGHP. In addition, it is found that the wick surface does not dry out even in the vertical posture at present experimental conditions.

Keywords: Heat spreader; postural effect; inner structure

1. Introduction

Recently, thermal management of electronic devices has been a great concern, because the poor cooling ability leads to various reliability problems and lower working efficiency in such devices. Particularly, lack in the cooling ability of a light-emitting diode (LED) substrate ruins the quality of lighting, because the light emitting efficiency of LEDs gets lowered with higher working temperature, which is caused mainly by its poor cooling ability resulting in non-uniform lighting performance. To solve such thermal management problems, a flat heat pipe such as vapor chambers would be one of the hopeful solutions because of their higher effective thermal conductivity in comparison to that of metal materials, and there has been a lot of studies on various types of vapor chambers (Boukhanouf et al. (2006), Koito et al. (2006(a), (b)), Xie et al. (2008), Wong et al. (2010, 2011)). For ordinary flat

doi:10.1016/j.phpro.2015.07.079

heat pipes, however, the gravitational force strongly affects the coolant distribution or circulation and their thermal performance. Thus, their thermal performance depends on their mounting orientation, which makes it difficult to utilize such kinds of flat heat pipes as a substrate of a LED array, because a LED light system can be installed in various orientations. Therefore, the orientational influence on thermal performance is a major drawback for such applications. To solve such problems of conventional vapor chambers, a novel flat heat pipe called FGHP (Fine Grid Heat Pipe) has been developed by Morex Kiire Co., Ltd. located in Kagoshima, Japan. In the previous study, it was found that the thermal performance of the FGHP is scarcely affected by its mounting orientation (Mizuta et al., 2013). Such characteristics is supposed to be achieved by the design of its inner structure which was made to diminish the influence of gravity on the coolant distributions inside the flat heat pipe, but the actual coolant distribution has not been experimentally estimated so far.

In this study, we utilized neutron radiography to clarify the postural effect on the coolant distribution in the FGHP heat spreader under the working conditions.

Nomenclature

c	Gain of the imaging system
G	Grey level of neutron image [-]
Q_{in}	Heat input to the FGHP sample [W]
R_{th}	Total thermal resistance [K/W]
T_a	Atmospheric temperature [K]
T_{sp}	Surface temperature of the heat spreader [K]
Greek	
δ	Effective material thickness along the neutron beam [cm]
ϕ_{th}	Thermal neutron flux [n cm^{-2} s^{-1}]
Σ	Macroscopic cross section [cm^{-1}]
Subscripts	
d	Dark current
VP	Vapor path
W	Water coolant
WK	Wick area

2. Experiments

2.1 Fine Grid Heat Pipe (FGHP) and experimental setup

Figure 1 shows a structure of the FGHP. All inner and outer structures such as wick, vapor path, and dimple are fabricated by fine etching technique to realize optimal coolant circulation. In general, the FGHP heat spreader is composed of several etched copper plates which are attached each other by vacuum hot press technique without any binder so as to avoid electric corrosion. The top and bottom plates have almost the same structure except injection holes of coolant. Both of them have dimple structures in their inner surfaces, which were designed to enhance boiling heat transfer at the bottom plate and to avoid film condensation at the top plate, respectively. Several middle plates are sandwiched by the top and bottom plates. Each middle plate has vapor path and wick area, for movement of vapor and return of condensed coolant, respectively. Pure water was utilized as a coolant for the test sample used in this experiment

Figure 2 shows a schematic of the coolant circulation in the FGHP. Under working conditions, heat applied to a small area through the bottom plate evaporates the working fluid. The resulting vapor travels through the vapor path to the entire area of the top plate, where the vapor condenses releasing its latent heat of vaporization to the heat sink. Then the condensate gets back to the bottom plate through the wick area by the capillary force.

Moreover, dimple structures of the top and bottom plates also induce capillary force, which enhance the coolant movement. The test sample of the FGHP heat spreader was 65×65×2 mm^3 and was set vertically as shown in Fig. 3. A ceramic heater of 25×25×1.75 mm^3 was attached to the central part of the bottom plate as a heat source, and the other side of the FGHP was cooled by three 35×35 mm^2 pin-fin type aluminum heat sinks. K-type thermocouples were used to measure the surface temperature of the heat spreader and the atmospheric temperature to calculate the thermal resistance of the FGHP by the following equation:

$$R_{th} = \frac{T_{sp} - T_a}{Q_{in}}. \tag{1}$$

where, R_{th} is the total thermal resistance [K/W], T_{sp} is the surface temperature of the bottom plate of the heat spreader [K], T_a is the atmospheric temperature [K], and Q_{in} is the power applied to the ceramic heater [W], respectively.

2.2 Neutron imaging and signal processing

The neutron imaging system used in this study is shown in Fig.4. A CCD camera (BU-53LN, BITRAN Co. Ltd.) was utilized, which has 4008×2672 pixels and ^{6}LiFZnS (50μm thickness) was used as a scintillator screen. The spatial resolution was 9.0 μm/pixel at the present system setup, however, the effective spatial resolution was about 50 μm/pixel due to the scintillator screen characteristics. The experiment was conducted at the E-2 port of the Kyoto University Research Reactor (KUR), where the thermal neutron flux at the sample position was about 3×10^5 n/cm^2s at 5 MW operation mode. Neutron imaging was performed at the 1 MW operation mode and the exposure time was 300 s in this study. To investigate the effect of gravity on the distribution of coolant, neutron radiography images were captured under various heating conditions. The intensity of the penetrated neutron beam at four different positions in the test sample was estimated from the neutron radiography images. The interrogation area for the calculation of the intensity was 44×170 pixels (about 0.4×1.5 mm), and the spatial averaged value was used to decrease the statistical noise. From the results, it was found that the intensity at the outside of the sample slightly changed during the experiments (ranged from 99.9 % to 101.2 % compared with the adiabatic condition). Thus, the intensity of the images was corrected by the image intensities at the reference points outside the sample.

To estimate the coolant distribution in the vapor path, the formulations of the neutron attenuations in the FGHP were derived. Neglecting the scattering components of the neutrons, the grey levels in the vapor path and the wick area can be expressed as follows:

$$G_{VP}(x,y) = c\phi_{th}(x,y)exp(-\Sigma_{Cu}\delta_{VP}) + G_d(x,y). \tag{2}$$

$$G_{WK}(x,y) = c\phi_{th}(x,y)exp\left(-\Sigma_{Cu}\delta_{WK} - \Sigma_W\delta_W(x,y)\right) + G_d(x,y). \tag{3}$$

where ϕ_{th} denotes the incident thermal neutron flux, c the gain of the imaging system, G the grey level, Σ the macroscopic cross section, δ the effective thickness along the neutron path. The subscripts *VP, WK, W* denote the vapor path, the wick area, and the water coolant, respectively. $G_d(x,y)$ is the dark current of the imaging system. Assuming the uniformity of the neutron beam profile, the difference in the incident neutron flux could be neglected in the above mentioned equations, if the two areas are adjacent to each other. Then, the following equation can be derived:

$$\frac{G_{WK}(x,y) - G_d(x,y)}{G_{VP}(x,y) - G_d(x,y)} = exp\left(-\Sigma_{Cu}(\delta_{WK} - \delta_{VP}) - \Sigma_W\delta_W(x,y)\right) \tag{4}$$

Then, the liquid thickness in the wick area can be estimated as follows:

$$\delta_W(x,y) = -ln\left(\frac{G_{WK}(x,y) - G_d(x,y)}{G_{VP}(x,y) - G_d(x,y)}\right)/\Sigma_W - \frac{\Sigma_{Cu}}{\Sigma_W}(\delta_{WK} - \delta_{VP}) \quad (5)$$

Here, the macroscopic cross section of water Σ_W is 3.47 cm^{-1}, and that of copper Σ_{Cu} is 0.924 cm^{-1}, respectively. In addition, the difference in the effective copper thickness $(\delta_{WK} - \delta_{VP})$ is about 0.1 mm for the present test sample. In the following discussions, the area averaged value of the film thickness in the wick area at four positions (top, bottom, left, and right) in the test sample as indicated in Fig. 3 (c).

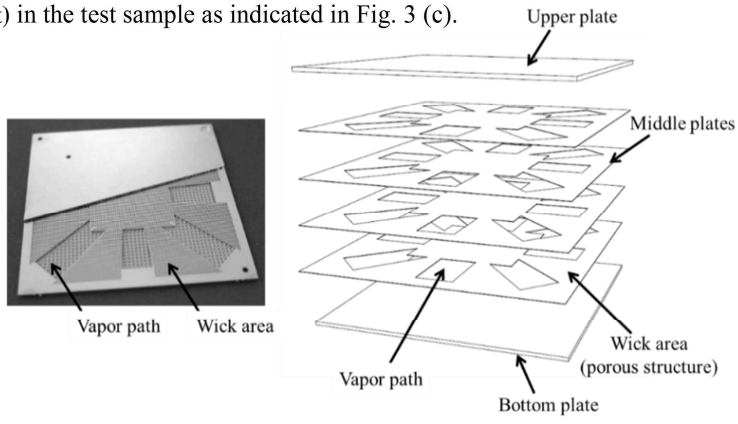

Fig. 1. Schematic diagram of FGHP (Fine Grid Heat Pipe) heat spreader.

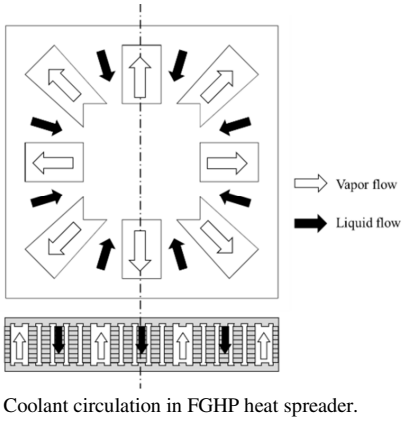

Fig. 2. Coolant circulation in FGHP heat spreader.

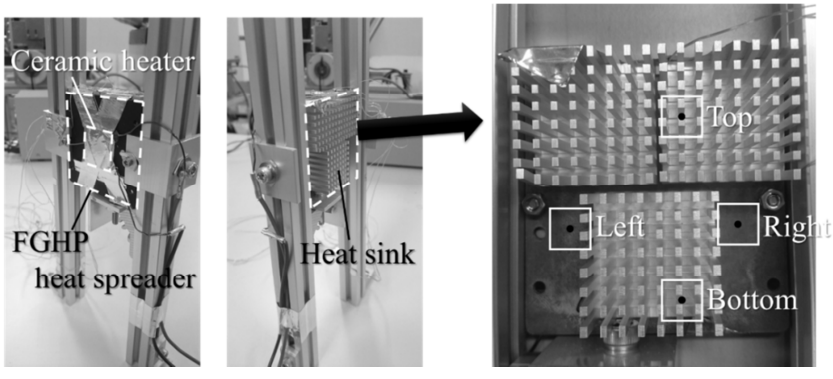

(a) Front side (b) Rear side (c) Measurement points

Fig. 3. Setup of test module.

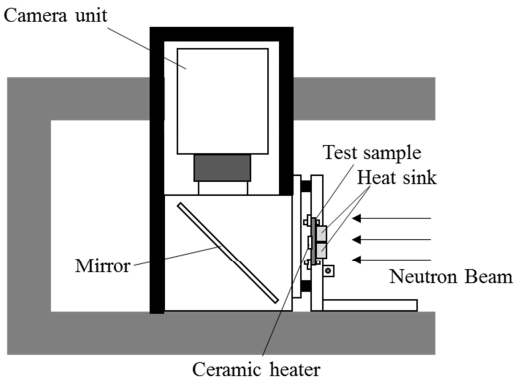

Fig. 4. Schematic diagram of the neutron imaging system and the test setup

3. Results

Figure 5 shows typical neutron image superimposed on the optical image of the test section. Inside black broken quadrate in each partial enlarged image denotes wick area, and the outside is the vapor path. As shown in this figure, the grey level in the wick area is smaller than that in the vapor path region. Figure 6 shows the magnified neutron images (about 1.94 mm square area) at each measurement point under various heating conditions. The heating conditions are summarized in Table 1. At the present experimental conditions, the heat input was varied from 0 to 15.1 W. As can be seen in these images, the coolant distributions seem to be almost constant regardless of the heating conditions. Under these conditions, thermal resistance, R_{th}, against heat input, Q_{in}, takes nearly constant value when Q_{in} is smaller than about 5 W, and begins to decrease with increasing Q_{in} as indicated in Fig. 7. This tendency may be attributed to the increase of the effective thermal conductivity of the FGHP as observed in the previous study (Mizuta et al., 2013).

The averaged values of the calculated liquid thickness in the wick area by eq. (5) are summarized in Table 1 along with the measured thermal resistance. Figure 8 shows the variation of the normalized spatial averaged grey level of each image and the measured liquid thickness in the wick area with Q_{in}. As shown in Fig. 8(a), the image intensities are normalized by those at $Q_{in} = 0$ (Run 0) and the normalized intensities take almost 1 regardless of Q_{in}, which indicates that the total amount of water in each area at all positions keep almost constant value compared to that under adiabatic condition.

As shown in Fig. 8(b), the measured values of liquid thickness in the wick area take the minimum at the top and the maximum at the bottom positions. The measured values range from 200 to 480 μm, becomes larger along the gravitational direction, and almost constant regardless of the heat input Q_{in}. From the design of the inner structure of the FGHP heat spreader, the maximum liquid thickness in the wick area is estimated as 0.6 mm (about 0.1 mm in the middle plates and 0.5 mm in the top and the bottom plates), therefore, at least 0.1 mm thick liquid layer covers the surface of the middle plates as the wick structure, which indicates that the surface of the wick area does not dry out under working conditions even at the top position.

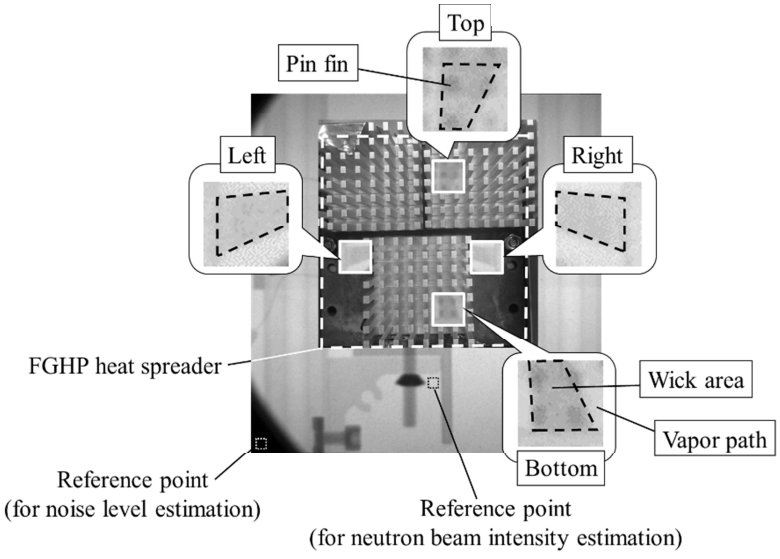

(a) Whole image

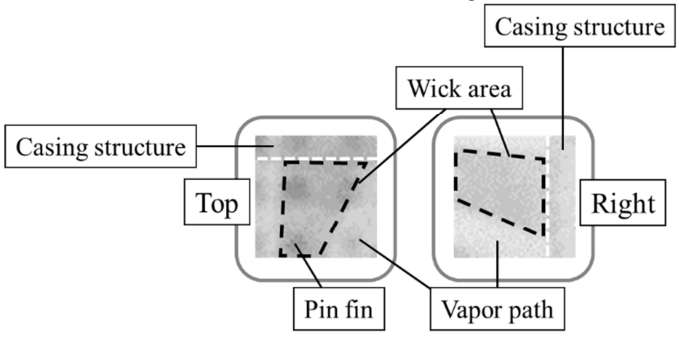

(b) Magnified images of top and right.

Fig.5. Typical neutron images superimposed on optical image.
(Inside black broken quadrate in each enlarged image denote the wick area, and the outside the vapor path.)

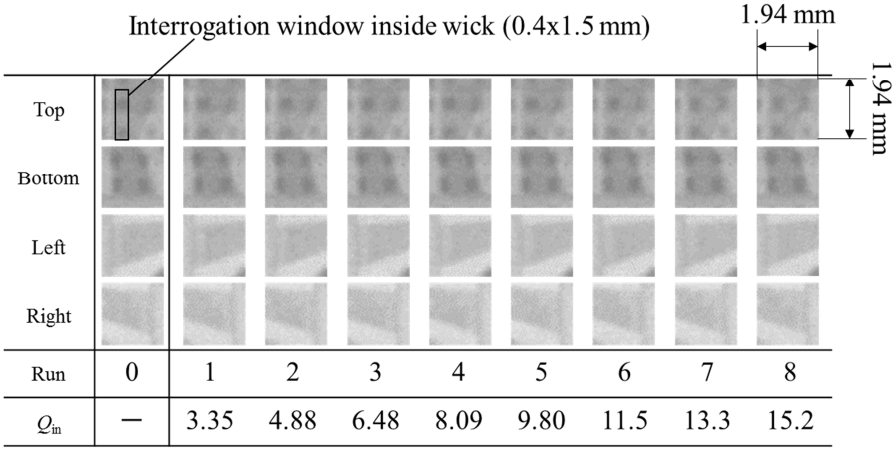

Run	0	1	2	3	4	5	6	7	8
Q_{in}	—	3.35	4.88	6.48	8.09	9.80	11.5	13.3	15.2

Fig. 6. Magnified neutron images at each point under various heating conditions.

Table 1. Experimental results.

Run	T_a [K]	T_{sp} [K]	Q_{in} [W]	The effective liquid film thickness in the wick area [mm]				R_{th} [K/W]
				Top	Bottom	Right	Left	
0	291.4	291.4	-	0.26	0.49	0.39	0.41	-
1	292.0	305.3	3.3	0.24	0.47	0.37	0.38	3.97
2	292.0	311.4	4.9	0.24	0.45	0.38	0.37	3.97
3	292.5	317.4	6.5	0.26	0.45	0.37	0.36	3.85
4	292.4	322.8	8.1	0.24	0.45	0.37	0.37	3.76
5	292.7	328.3	9.8	0.22	0.46	0.37	0.38	3.63
6	292.7	333.6	11.5	0.23	0.43	0.37	0.37	3.54
7	292.7	338.8	13.3	0.19	0.44	0.38	0.37	3.46
8	292.7	343.9	15.1	0.22	0.44	0.36	0.37	3.38

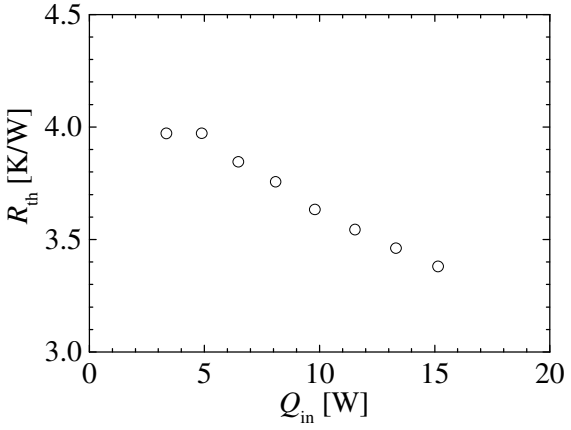

Fig. 7. Variation of thermal resistance with heat input.

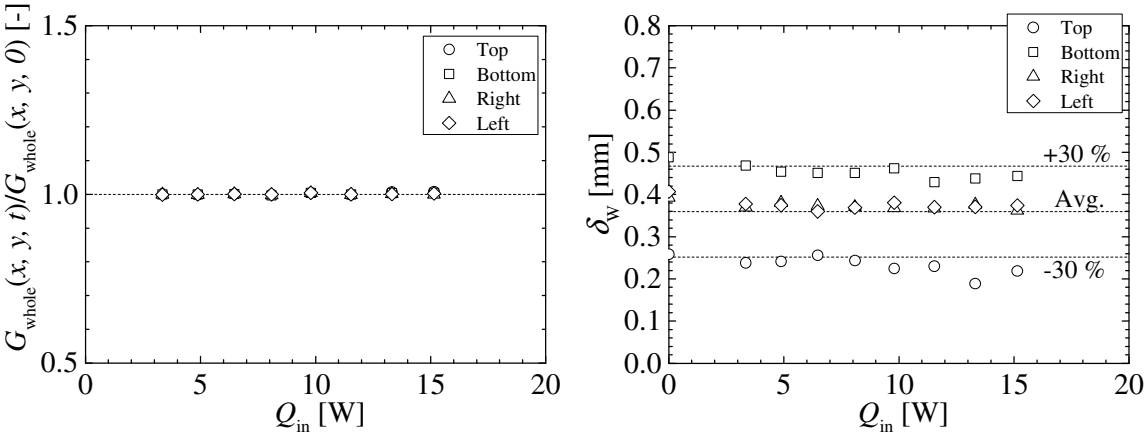

(a) Normalized image intensities at whole area in the partial image (b) liquid thickness in the wick area

Fig. 8. Variation of grey level and liquid thickness in the wick area with input power.

Conclusions

We have utilized neutron radiography to evaluate the coolant distribution in a newly developed flat heat pipe called FGHP^{TM} which has been designed to weaken the gravity effects on coolant distribution even if installed in vertical posture. Heat transfer experiments were also performed with neutron radiography. By the image processing of the neutron images, the liquid thickness was calculated in the vapor path at four different positions (top, down, right, and left) in the vertical posture. The measured liquid thickness was varied from 200 to 400 μm affected by the gravitational force and also by the heat input at the present experimental conditions. However, from the measurement results, it was found that the wick surface was covered by liquid layer even under the working conditions, which would support the facts found in the previous study that the FGHP can work even in the vertical posture.

References

Boukhanouf, R. et al., Experimental investigation of a flat plate heat pipe performance using IR thermal imaging camera, Applied Thermal Engineering, 26 (2006) 2148–2156.

Koito, Y. et al. (a), Fundamental Experiments and Numerical Analyses on Heat Transfer Characteristics of a Vapor Chamber (Effect of Heat Source Size), JSME International Journal, Series B., 49 (4) (2006) 1233-1240.

Koito, Y. et al. (b), Numerical analysis and experimental verification on thermal fluid phenomena in a vapor chamber, Applied Thermal Engineering, 26 (2006) 1669-1676.

Mizuta, K. et al., High-performance cooling system using novel heat pipe heat spreader, Proceeding of Japan-Taiwan Bilateral Workshop on Nano-Science 2013, Kagoshima.

Wong S. C. et al., A novel vapor chamber and its performance, International Journal of Heat and Mass Transfer, 53 (2010) 2377-2384.

Wong S. C. et al., Performance tests on a novel vapor chamber, Applied Thermal Engineering, 31 (2011) 1757-1762.

Xie X. L. et al., An experimental investigation on a novel high-performance integrated heat pipe–heat sink for high-flux chip cooling, Applied Thermal Engineering, 28 (2008) 433-439.